

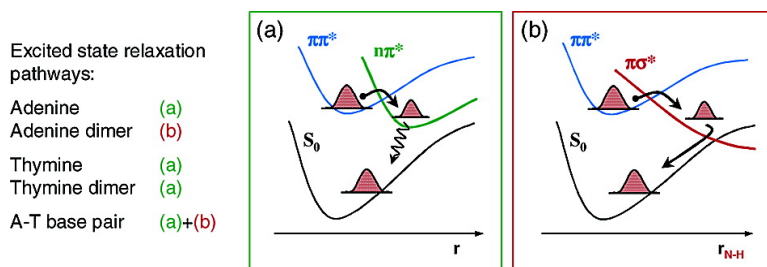
Article

Dynamics of Photoinduced Processes in Adenine and Thymine Base Pairs

E. Samoylova, H. Lippert, S. Ullrich, I. V. Hertel, W. Radloff, and T. Schultz

J. Am. Chem. Soc., **2005**, 127 (6), 1782-1786 • DOI: 10.1021/ja044369q • Publication Date (Web): 19 January 2005

Downloaded from <http://pubs.acs.org> on March 24, 2009



More About This Article

Additional resources and features associated with this article are available within the HTML version:

- Supporting Information
- Links to the 14 articles that cite this article, as of the time of this article download
- Access to high resolution figures
- Links to articles and content related to this article
- Copyright permission to reproduce figures and/or text from this article

[View the Full Text HTML](#)

Dynamics of Photoinduced Processes in Adenine and Thymine Base Pairs

E. Samoylova,[†] H. Lippert,[†] S. Ullrich,^{‡§} I. V. Hertel,[†] W. Radloff,[†] and T. Schultz[†]

Contribution from the Max-Born-Institut, Max-Born-Str. 2a, D-12489 Berlin, Germany, and Steacie Institute for Molecular Sciences, National Research Council of Canada, 100 Sussex Drive, Ottawa, Ontario, Canada K1A 0R6

Received September 16, 2004; E-mail: schultz@mbi-berlin.de

Abstract: The excited-state dynamics of adenine and thymine dimers and the adenine–thymine base pair were investigated by femtosecond pump–probe ionization spectroscopy with excitation wavelengths of 250–272 nm. The base pairs showed a characteristic ultrafast decay of the initially excited $\pi\pi^*$ state to an $n\pi^*$ state (lifetime $\tau^{n\pi^*} \approx 100$ fs) followed by a slower decay of the latter with $\tau^{n\pi^*} \approx 0.9$ ps for (adenine)₂, $\tau^{n\pi^*} = 6$ –9 ps for (thymine)₂, and $\tau^{n\pi^*} \approx 2.4$ ps for the adenine–thymine base pair. In the adenine dimer, a competing decay of the $\pi\pi^*$ state via the $\pi\sigma^*$ state greatly suppressed the $n\pi^*$ state signals. Similarities of the excited-state decay parameters in the isolated bases and the base pairs suggest an intramonomer relaxation mechanism in the base pairs.

Introduction

The abundance of ultraviolet radiation in sunlight requires an extraordinary photostability of deoxy-nucleic acid (DNA), the carrier of genetic information, to protect it against chemical reactions with potentially mutagenic or carcinogenic consequences. The evolutionary choice of four building blocks of DNA: adenine, thymine, guanine and cytosine, may thus be closely connected to their photochemical properties. High photostability is roughly equivalent to short excited-state lifetimes, and this work describes an investigation of the ultrafast relaxation dynamics and relaxation pathways in the isolated DNA bases adenine (A) and thymine (T), the corresponding dimers (A₂, T₂), and the adenine–thymine (A–T) base pair.

Extensive theoretical and experimental studies were performed to elucidate the electronic structure of the four isolated bases and the base pairs (see, e.g., ref 1 and references therein). Following a reductionist approach, many experiments focused on the isolated bases in a molecular beam, revealing basic information about their energetics and geometries. Frequency resolved studies of fluorescence and multiphoton ionization were restricted to wavelength regions close to the UV absorbing $\pi\pi^*$ electronic transition of the bases, i.e., where only little excess vibrational energy was deposited in the molecule. Only here, longer living vibronic states allowed the spectroscopic analysis with high spectral resolution as necessary for the selective study of closely spaced features. For the dominant 9H-tautomer of A, for example, spectra were recorded near to the reported origin of the $n\pi^*$ and the $\pi\pi^*$ state at 35 497 cm⁻¹ and 36 105 cm⁻¹.^{2,3}

Larger excitation energies led to diffuse spectral structures, which may be caused by ultrashort lifetimes of the corresponding excited states. For A, such a diffuse structure was observed at ≥ 1200 cm⁻¹ above the origin transition frequency to the lowest electronic $n\pi^*$ state.² In those spectral regions, femtosecond time-resolved studies can yield energetic as well as dynamic information.

First time-resolved experiments applied picosecond (ps) and femtosecond (fs) pump–probe techniques to the A and T monomers prepared in a molecular beam. Lührs and co-workers observed an excited-state lifetime of 9 ps after excitation of A with ps laser pulses at 277 nm,⁴ within the region of sharp absorption bands. Using fs pulses at 267 nm (the region of diffuse bands), Kang and co-workers found a lifetime of 1 ps for A⁵ and 6.4 ps for T.⁶ Ullrich and co-workers provided a detailed analysis of the photoelectron spectra of A excited at 250 or 266 nm and demonstrated that the picosecond signal decay (here with a time constant of 0.75 ps) was preceded by a much shorter contribution of ≤ 50 fs, the detection of which was limited by the time resolution of their experiment.⁷ The interpretation of the two time constants was based on the identification of the excited-state characters via their photoelectron spectra and correlated well with the potential energy scheme of A calculated by Sobolewski and Domcke⁸ (Figure 1). The ultrafast decay (≤ 50 fs) was assigned to internal

[†] Max-Born-Institut.

[‡] Steacie Institute for Molecular Sciences.

[§] Currently at University of Georgia, Department of Physics and Astronomy, Athens, Georgia 30602.

(1) Crespo-Hernandez, C. E.; Cohen, B.; Hare, P. M.; Kohler, B. *Chem. Rev.* **2004**, *104*, 1977.

(2) Kim, N. J.; Jeong, G.; Kim, Y. S.; Sung, J.; Kim, S. K. *J. Chem. Phys.* **2000**, *113*, 10051.

(3) Nir, E.; Plützer, C.; Kleinermanns, K. *Eur. Phys. J. D* **2002**, *20*, 317.

(4) Lührs, D. C.; Viallon, J.; Fischer, I. *Phys. Chem. Chem. Phys.* **2001**, *3*, 1827.

(5) Kang, H.; Jung, B.; Kim, S. K. *J. Chem. Phys.* **2003**, *118*, 6717.

(6) Kang, H.; Lee, K. T.; Jung, B.; Ko, Y. J.; Kim, S. K. *J. Am. Chem. Soc.* **2002**, *124*, 12958.

(7) Ullrich, S.; Schultz, T.; Zgierski, M. Z.; Stolow, A. *J. Am. Chem. Soc.* **2004**, *126*, 2262.

(8) Sobolewski, A. L.; Domcke, W.; Dedonder-Lardeux, C.; Jouvet, C. *Phys. Chem. Chem. Phys.* **2002**, *4*, 1093.

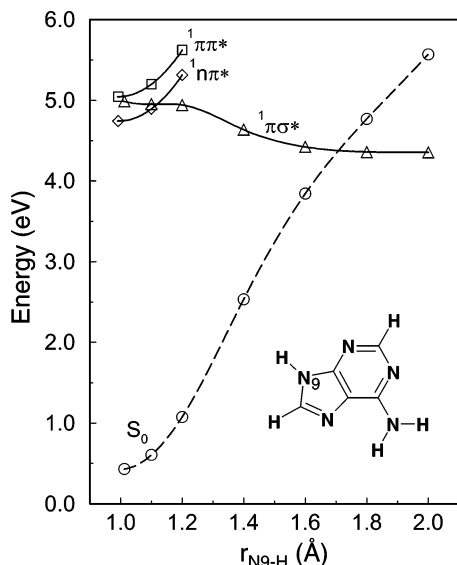


Figure 1. Ab initio calculated potential energy curves of adenine with respect to the N–H coordinate, according to ref 8.

conversion from the initially excited $\pi\pi^*$ state to the $n\pi^*$ state and the $\pi\sigma^*$ state. Both of the latter states decay through nonadiabatic coupling to the electronic ground state. The longer lifetime of 0.75 ps was assigned as the lifetime of the $n\pi^*$ state, whereas the $\pi\sigma^*$ state displayed no measurable lifetime. Nanosecond experiments confirmed the population of the $\pi\sigma^*$ state by the detection of H atoms, which presumably result from the dissociation of A along the N–H bond on the repulsive $\pi\sigma^*$ potential energy surface.^{9,10}

For the hydrogen-bonded base pairs, additional excited-state processes may occur and could dominate the excited-state relaxation. Several processes were investigated with the help of model compounds: a double proton-transfer reaction was studied in the azaindole dimer.¹¹ This reaction did not, however, lead to short excited-state lifetimes, and the observed fluorescence stands in stark contrast to the low fluorescence of DNA bases and base pairs. An electron–proton transfer reaction from a locally excited (LE) $\pi\pi^*$ state to a charge transfer (CT) $\pi\pi^*$ state was suggested based on theoretical investigations of the model system 2-aminopyridine dimer.¹² The existence of this reaction was recently confirmed by a femtosecond pump–probe experiment,¹³ where a greatly accelerated excited-state relaxation was observed for the hydrogen-bound dimer. Alternatively, a single hydrogen transfer might proceed on the $\pi\sigma^*$ potential surface, favored by the lowering of the barrier between the $\pi\pi^*$ and $\pi\sigma^*$ states as predicted theoretically for hydrogen-bonded clusters.¹⁴ In both cases, via the $\pi\sigma^*$ as well as via the $\pi\pi^*$ (CT) state, a H-transfer reaction can mediate the relaxation of the initially excited $\pi\pi^*$ (LE) state to the electronic ground state and significantly alter the excited-state relaxation and photostability of the hydrogen bonded cluster.

In the present paper, we studied the dynamics of the homo- and heterodimers of A and T in the wavelength region of 250–

272 nm, i.e., in the energy range where the excited vibronic states of the monomers have short lifetimes. The band origins in the dimer spectra are red-shifted with respect to the monomers, and we excite the base pairs at somewhat enlarged excess energies, well within the region of diffuse spectral bands. The reported red-shift with respect to the $\pi\pi^*$ origin of the 9H-adenine at $36\,105\text{ cm}^{-1}$ is about 1000 cm^{-1} for A_2 ¹⁵ and about 1050 cm^{-1} for A–T.¹⁶

Experimental Setup

Samples of DNA bases in glass or aluminum holders were evaporated in a stainless steel oven at 200–220 °C. The bases were coexpanded with a carrier gas in a supersonic jet expansion through a pulsed valve (General Valve series 9, modified for temperatures $\leq 300\text{ °C}$). As carrier gas, we employed ≤ 1.6 bar of helium or 0.6–0.8 bar of argon for narrow or broad cluster distributions, respectively. The molecular beam was skimmed and crossed with two copropagating laser beams for molecular excitation and ionization. The ions were mass-analyzed in a time-of-flight mass spectrometer.

The laser system employed was a commercial Ti:Sapphire oscillator, regeneratively amplified to mJ levels at 1 kHz (Spectra Physics TSUNAMI and SPITFIRE or Clark MXR). For the excitation pulses, part of the beam was sent through an optical parametric amplifier (Light Conversion TOPAS, model 4/800/f) and subsequently frequency mixed and frequency doubled to give $\leq 2\text{ }\mu\text{J}$ of tunable light in the wavelength range 250–272 nm, or we used the third harmonic radiation at 266 nm. For the ionization pulses, up to 160 μJ of the 800 nm beam was used directly or frequency doubled to give 70 μJ pulses of 400 nm light. The beams were further attenuated with neutral density filters by factors of 3–30 and focused to spot sizes of 100–200 μm . In all cases, the fluence of the pump pulses was restricted to values below 10 mJ/cm^2 to avoid multiphoton excitation and the probe pulse intensity was $< 3 \times 10^{11}\text{ W/cm}^2$ to avoid strong field effects in the ionization step. The temporal width of the laser pulses was approximately 140 fs.

To obtain time-dependent ion signals, a delay line with submicrometer resolution was used to scan the time delay Δt between the excitation and ionization pulses. The observed signals are directly proportional to the excited-state populations; i.e., the measured decay of an ion signal as a function of Δt is a direct measure of the corresponding excited state population decay. Typically eight or more scans with alternating scan direction were averaged to avoid systematic errors from long-term instabilities of the laser system or the cluster source.

Results

A fairly complex mass spectrum was obtained upon coexpansion of A and T with 0.6 bar of argon (Figure 2a). The most prominent signals were observed for the A and T monomers and dimers, as well as the A–T heterodimer. Smaller signals were detected for trimers and tetramers and for products from molecular fragmentation processes. The time-dependent ion signals corresponding to the cluster spectrum in Figure 2a show a biexponential decay of the A and A_2 signals (Figures 2b,c). The time-dependent signals were fitted with a stepwise kinetic model $B \xrightarrow{\tau_1} C \xrightarrow{\tau_2} \text{dark state}$, assuming an exponential population decay (lifetime τ_1) for state B and a corresponding rise (τ_1) and subsequent decay (τ_2) for state C. For an accurate fit, we had to account for two additional sources of signal: an inverted process, i.e., excitation with 800 nm and ionization with 272 nm, resulted in a small signal for negative delays,

(9) Hünig, I.; Plützer, C.; Seefeld, K. A.; Löwenich, D.; Nispel, M.; Kleiner-manns, K. *Chem. Phys. Chem.* **2004**, *5*, 1427.
 (10) Zierhut, M.; Roth, W.; Fischer, I. *Phys. Chem. Chem. Phys.* **2004**, *6*, 5178.
 (11) Douhal, A.; Kim, S. K.; Zewail, A. H. *Nature* **1995**, *378*, 260.
 (12) Sobolewski, A. L.; Domcke, W. *Chem. Phys.* **2003**, *294*, 73.
 (13) Schultz, T.; Samoylova, E.; Radloff, W.; Hertel, I. V.; Domcke, W. *Science* **2004**, *306*, 1765.
 (14) Sobolewski, A. L.; Domcke, W. *Eur. J. Phys. D* **2002**, *20*, 369.

(15) Plützer, C.; Hünig, I.; Kleiner-manns, K. *Phys. Chem. Chem. Phys.* **2003**, *5*, 1158.
 (16) Plützer, C.; Hünig, I.; Kleiner-manns, K.; Nir, E.; de Vries, M. S. *Phys. Chem. Chem. Phys.* **2003**, *4*, 838.

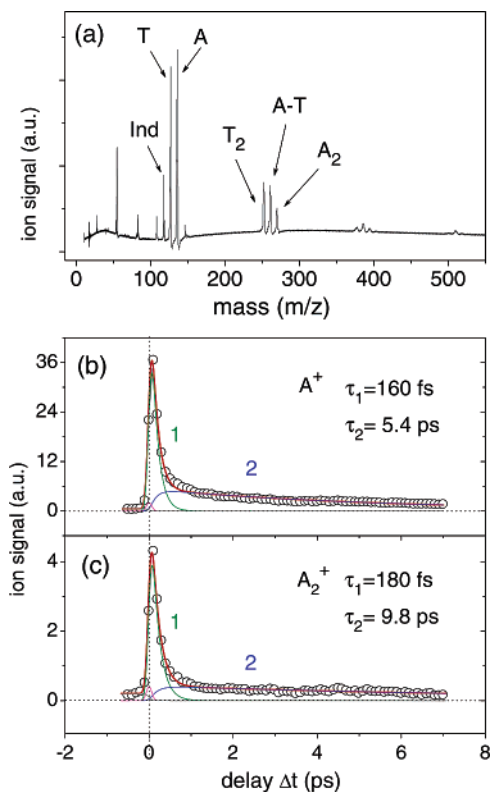


Figure 2. (a) Mass spectrum of a broad cluster distribution of adenine (A) and thymine (T) clusters obtained for 272 nm excitation and 800 nm ionization. A small amount of indole (Ind) was added for calibration purposes. (b, c) The ion signals of A (b) and A_2 (c) as a function of the delay time Δt . The theoretical fit curve (heavy line) is the sum of four contributions (thin lines), two of which are characterized by the time constants τ_1 and τ_2 (see text for details). All signals are given in arbitrary units (a.u.), but proportionality of the signals is conserved.

and a small nonresonant signal contributed within the pump–probe laser overlap, symmetrical to $\Delta t = 0$.

In the broad cluster distribution shown in Figure 2, the theoretical fit curves for both signals showed an ultrafast contribution with the time constant $\tau_1 \approx 170$ fs and a longer-living contribution with τ_2 on the order of 5–10 ps. This was in contradiction to the reported 1 ps lifetime for A at this wavelength.^{2,7} We assigned this discrepancy to artifacts caused by the fragmentation of larger clusters. The ratio of the signal maxima for A^+/A_2^+ or T^+/T_2^+ in Figure 2 is a measure of the width of the cluster distribution and is 9 and 3, respectively. In further measurements, we strongly reduced the width of the cluster distribution to remove larger clusters with $n \geq 3$ from the molecular beam, thus removing the artifactual contributions. In Figures 3–5, the ratio of the signal maxima was $A^+/A_2^+ \geq 60$ and the A dynamics agreed well with results in the literature.

The excited-state dynamics for A and A_2 , excited at 263 nm and ionized at 400 nm, are shown in Figure 3. On the left-hand side, the ion signals are shown with high time resolution to allow the determination of the fast time constant $\tau_1 = 90 \pm 20$ fs for A and $\tau_1 = 75 \pm 30$ fs for A_2 . To obtain reliable values for the short τ_1 lifetimes, the delay time zero was determined in the same experiment via the pump–probe signal of indole. Nevertheless, the uncertainty of the τ_1 values obtained by the fit procedure was relatively large, on the order of ± 30 fs, due to the limited time resolution of our experiments and the moderate signal-to-noise ratio. Longer pump–probe scans allowed the

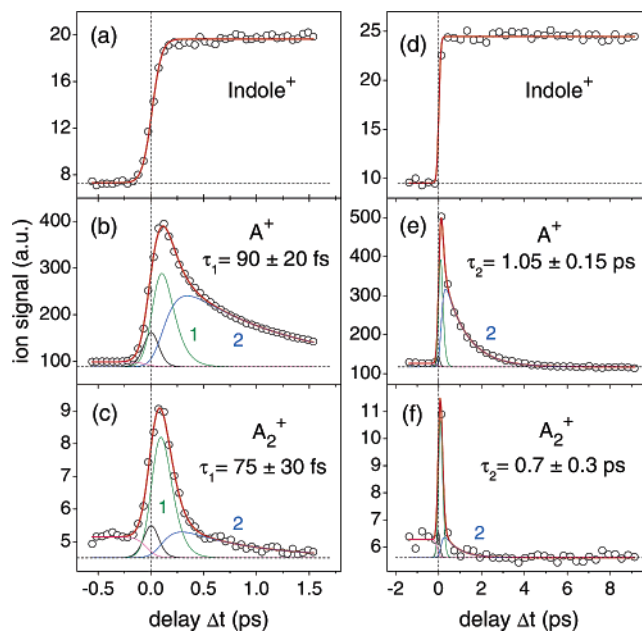


Figure 3. Ion signals of indole, adenine, and adenine dimer as a function of the delay time Δt between the pump (263 nm) and the probe (400 nm) pulses. The scales of the ordinates in scans a–f reflect the relative magnitudes of the signals and illustrate the narrow cluster distribution in this experiment. Short delay scans (left) and longer delay scans (right) were performed to characterize the femtosecond and picosecond dynamics, respectively. The fit curves (lines) were obtained as described in Figure 2.

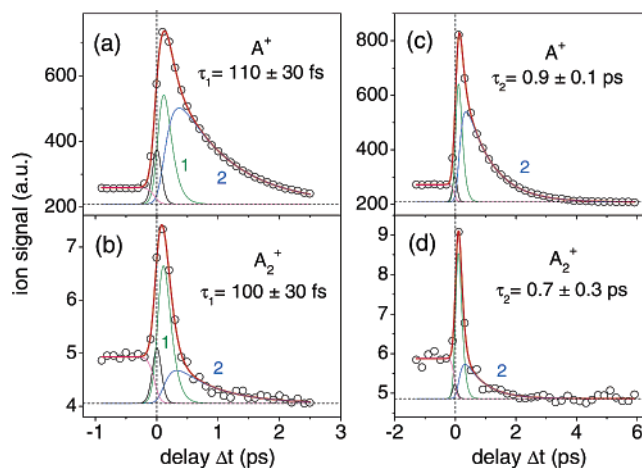


Figure 4. Ion signals of adenine and adenine dimer as a function of the delay time Δt between the pump (250 nm) and the probe (400 nm) pulses. The fit curves (lines) were obtained as described in Figure 2.

determination of a second time constant $\tau_2 = 1.05 \pm 0.15$ ps for A and $\tau_2 = 0.7 \pm 0.3$ ps for A_2 (Figure 3, right-hand side). An inverted process, i.e., excitation with 400 nm and ionization with 263 nm, resulted in a small signal for negative delays and a small nonresonant signal contributed within the pump–probe laser overlap close to $\Delta t = 0$.

Excitation with higher energy pump photons at 250 nm gave near identical results to those described above (Figure 4). The fit procedure revealed time constants $\tau_1 \approx 100$ fs and $\tau_2 \approx 0.8$ ps for A and A_2 , equal to those measured for 263 nm within the limits of experimental errors.

In addition to the A cluster dynamics, we investigated the dynamics of T clusters and the A–T base pair, excited at $\lambda_{pu} = 272$ nm and ionized at $\lambda_{pr} = 800$ nm (Figure 5). The time constants τ_1 and τ_2 of A and A_2 agree with the values at the

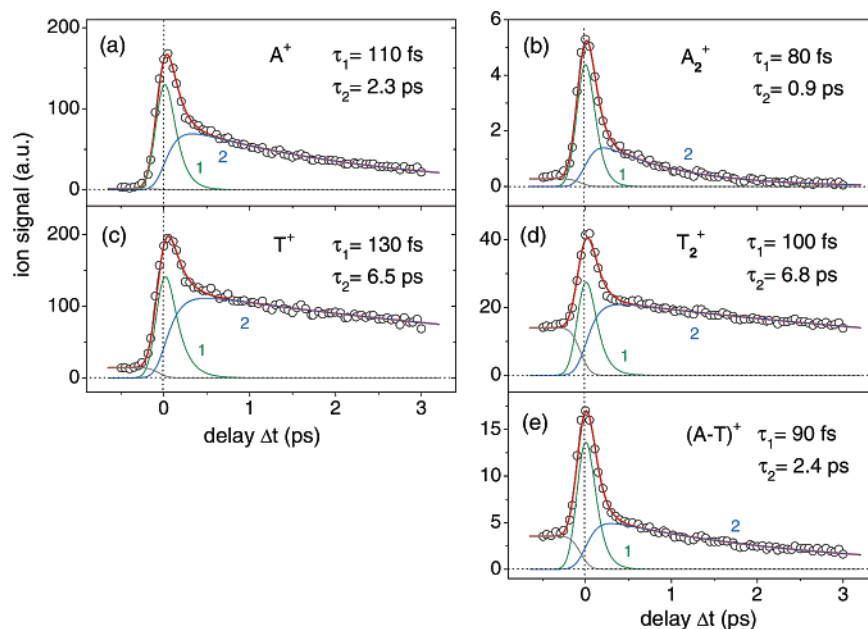


Figure 5. Ion signals of the adenine and thymine monomers and dimers as a function of the delay time Δt between the pump (272 nm) and the probe (800 nm) pulses. Background signals due to pump only and probe only ionization processes were subtracted. The width of the cluster distribution is narrow as demonstrated by the ratio of the adenine monomer to dimer signals $A^+/A_2^+ \approx 60$. The fit curves (lines) were obtained as described in Figure 2. The longer lifetimes $\tau_2 = 6\text{--}9$ ps for thymine were confirmed by longer pump–probe scans with delay times of up to 40 ps.

pump wavelengths of 263 nm and 250 nm (Figures 3, 4) except for the somewhat larger value of $\tau_2 = 2.3$ ps for A. For T, we found identical dynamics for the monomer and all clusters up to a size of $n \leq 8$ (not shown here). The lifetimes of $\tau_1 = 110 \pm 30$ fs, $\tau_2 = 6\text{--}9$ ps were similar to those described in the literature for the monomer.^{2,7} The dynamics of the A–T base pair with $\tau_1 = 90 \pm 30$ fs and $\tau_2 = 2.4 \pm 1$ ps were between those observed for the A_2 and T_2 homodimers. The relatively large constant signals at delay times $\Delta t < 0$ reflect a population of long-living states by the 800 nm laser pulses.

Discussion

Comparing the dynamics obtained for A and A_2 for a broad (Figure 2) and a narrow (Figures 3–5) cluster distribution, we found a strong elongation of the τ_2 decay time for the former. This was caused by the fragmentation of the larger clusters ($n \geq 3$) in the neutral and/or ionic states, which led to additional signal contributions in the monomer and dimer mass channels.¹⁷ Hence, undistorted excited state dynamics for the monomer and dimer could only be measured for narrow cluster distributions (Figures 3–5). Similar conclusions have been drawn in other cluster studies, i.e., the analysis of ammonia clusters.¹⁸ Unfortunately, this limited our investigation to the monomers and dimers and a mass-selective study of the larger clusters failed.

The lifetime $\tau_2 \approx 0.9$ ps found for A in the narrow cluster distribution agreed well with the results of Ullrich et al.⁷ and Kang et al.,⁵ measured in a cluster-free molecular beam and with similar excitation wavelengths. The independent determination of the delay time zero in our experiments allowed the clear identification of an ultrafast contribution with the lifetime $\tau_1 \approx 100$ fs, which was not observed by Kim. According to the potential energy surfaces (Figure 1) and in agreement with the

results of Ullrich et al., τ_1 was attributed to an internal conversion from the initially excited $\pi\pi^*$ to the lower lying $n\pi^*$ state and thus corresponds to the lifetime of the $\pi\pi^*$ state ($\tau_{1,\pi\pi^*}$). The large signal observed for the $n\pi^*$ state indicated that this is the dominant relaxation channel in A and that other decay channels play only a minor role. However, the presence of a possibly minor relaxation channel via the $\pi\sigma^*$ state was suggested repeatedly by theory,¹² time-resolved photoelectron spectroscopy,⁷ and the recent observation of neutral hydrogen fragments in nanosecond experiments.^{9,10} As the $\pi\sigma^*$ state population reveals no measurable lifetime, the observed longer time constant τ_2 corresponds to the lifetime of the $n\pi^*$ state ($\tau_{2,n\pi^*}$). This time constant reflects the subsequent nonadiabatic transition from the $n\pi^*$ state to the electronic ground state.

This interpretation was confirmed by the different behavior of A_2 : as observed in Figures 3 and 4, the magnitude of the $n\pi^*$ signal compared to the $\pi\pi^*$ signal was much smaller for A_2 than for A, while the corresponding lifetimes τ_1 and τ_2 remained unchanged. This indicated the presence of another decay channel, which competed with the $\pi\pi^* \rightarrow n\pi^*$ relaxation in the dimer and thus reduced the yield in the $n\pi^*$ state. First theoretical studies for the hydrogen-bonded dimer showed that the diffuse σ^* orbital is strongly stabilized for both the azine (ring NH) and the amino (NH_2) group in the cluster.¹⁹ This may lead to a stronger coupling between the $\pi\pi^*$ and $\pi\sigma^*$ states for the “inner” hydrogen bond N–H bonds as well as for the “outer” peripheric N–H bonds. Hence, for A_2 , relaxation via the $\pi\sigma^*$ state should be preferred compared to relaxation via the $n\pi^*$ state. No appreciable signal from the $\pi\sigma^*$ state was observed in our data, which agrees with the expectation of a very short lifetime due to the repulsive character of this state along the N–H bond (see Figure 1). The existence of the “inner” $\pi\sigma^*$ relaxation channel was also suggested by the detection of A–H radicals after excitation with ns laser pulses.⁹ These

(17) Dedonder-Lardeux, C.; Grosswasser, D.; Jouvet, C.; Martrenchard, S.; Teahn, A. *Phys. Chem. Chem. Phys.* **2001**, *3*, 4316.

(18) Farmanara, P.; Radloff, W.; Stert, V.; Ritze, H.-H.; Hertel, I. V. *J. Chem. Phys.* **1999**, *111*, 633.

(19) Ritze, H.-H. Private communication.

fragmentation products were assigned to an H-transfer in the excited dimer, followed by asymmetric fragmentation.

Investigating the wavelength dependence of the A and A₂ signals, we found no significant changes of the lifetime $\tau_{1,\pi\pi^*} = 90 \pm 30$ fs among $\lambda_{\text{pu}} = 250, 263,$ and 272 nm. The similarities of monomer and dimer indicate a comparable relaxation channel in both cases. The $n\pi^*$ lifetime $\tau_{2,n\pi^*} = 0.9 \pm 0.3$ ps remained constant between 250 and 263 nm but increased to $\tau_{2,n\pi^*} = 2.3$ ps for A at 272 nm. This increase in lifetime coincides nicely with the transition from sharp to broad spectral features observed in two-photon ionization spectra.² For an even longer excitation wavelength of 277 nm, Lührs and co-workers reported a 9 ps lifetime.⁴ Due to the red-shifted absorption band in the dimer, we did not observe a prolongation of the $n\pi^*$ lifetime in A₂ at 272 nm.

In T, the energy gap between the low-lying $n\pi^*$ state and the $\pi\sigma^*$ state is significantly larger than in A, due to the lower energy of the $n\pi^*$ state¹. Hence, the $\pi\sigma^*$ state fails to offer a competing relaxation channel, even if energetically stabilized in the dimer or larger clusters and the relaxation proceeds preferentially via the lower lying $n\pi^*$ state. This was reflected in our spectra: comparing the dynamics of T and T₂ (Figures 5c and 5d), we observed no significant change for the ratio of $n\pi^*$ and $\pi\pi^*$ signals. This result is in stark contrast to the observed reduction of the $n\pi^*$ contribution observed for the A dimer.

The A–T base pair showed similar excited state dynamics to those of the A and T homodimers (Figure 5). We interpreted this as evidence for a fairly unperturbed relaxation of the two chromophores in the A–T base pair, proceeding via the $\pi\pi^*$, $n\pi^*$, and $\pi\sigma^*$ states as observed for the monomers and homodimers. We detected no significant long-time signals above 20 ps even though we expect reasonable Franck–Condon factors for the ion detection of possible long-living secondary states. We therefore conclude that the relaxation to the electronic ground state should be complete on the picosecond time scale. With respect to the different isomers observed spectroscopically for the dimers in the molecular beam,¹⁶ we have to state that our experiments did not allow an isomer-selective study due to the large spectral width of the fs laser pulses. Instead, our time-dependent signals represent the sum of contributions from all isomers. While the lack of isomer discrimination is regrettable, the integral detection of all isomers does have advantages when compared with the difficulty to observe short-lived states in spectroscopic studies with ns pulses.

So far, we restricted our discussion to the dynamical processes involving the $\pi\pi^*$, $n\pi^*$, and $\pi\sigma^*$ states in the corresponding

monomers. In this, we have focused on intramonomer process dynamics where the excitation and relaxation proceeds within one of the two monomers and the other molecule interacts only by shifting the relative state energies. The lack of significant differences between the monomer and cluster dynamics support this interpretation. Other possible relaxation pathways which are specific to the clusters should be mentioned however and may play a role in certain cluster isomers. One such pathway involves a charge transfer from the initial, locally excited $\pi\pi^*$ state to a charge transfer $\pi\pi^*$ state as observed for the model chromophore 2-aminopyridine dimer.¹³ Another is a double proton transfer discussed extensively in the literature and demonstrated for the model chromophore azaindole dimer.¹¹ The combination of pump–probe spectroscopy with isomer selection methods, e.g., hole-burning, may be necessary to investigate the existence of such processes.

Conclusions

Femtosecond pump–probe spectroscopy of the isolated A and T bases confirmed a two-step relaxation mechanism of the optically active $\pi\pi^*$ state via a dark $n\pi^*$ state. A competing relaxation pathway via the $\pi\sigma^*$ state was found to play a dominant role in A₂, but not in T₂. This was explained by the relative energies and the resulting coupling of the three states and a stabilization of the $\pi\sigma^*$ state in the clusters. The excited state dynamics of the A–T base pair were similar to those of the homodimers and indicated a conserved relaxation mechanism in the two chromophores (intramonomer process). We found no evidence for relaxation pathways which would be specific for the A–T base pairs, such as intermolecular electron or proton transfer. More complex experiments, such as femtosecond time-resolved photoelectron spectroscopy and the isomer-selective measurement of base pair dynamics, are planned to conclusively prove the existence or absence of such pathways.

Acknowledgment. We thank Dr. F. Noack for his support by providing the laser system in the femtosecond application laboratory of the Max-Born-Institut Berlin. Financial support by the Deutsche Forschungsgemeinschaft through SFB-450 is gratefully acknowledged. S. Ullrich thanks Albert Stolow, the Femtosecond Science Program at the National Research Council of Canada, and the MBI for travel support. S.U. also acknowledges financial support from a Feodor Lynen Fellowship of the Alexander von Humboldt Foundation.

JA044369Q